



HAL
open science

The far-infrared spectrum of ^{18}O enriched water vapour (40–700 cm^{-1})

S.N. Mikhailenko, S. Béguier, T.A. Odintsova, M.Yu. Tretyakov, O. Pirali, A.
Campargue

► **To cite this version:**

S.N. Mikhailenko, S. Béguier, T.A. Odintsova, M.Yu. Tretyakov, O. Pirali, et al.. The far-infrared spectrum of ^{18}O enriched water vapour (40–700 cm^{-1}). *Journal of Quantitative Spectroscopy and Radiative Transfer*, 2020, 253, pp.107105. 10.1016/j.jqsrt.2020.107105 . hal-03078458

HAL Id: hal-03078458

<https://hal.science/hal-03078458>

Submitted on 16 Dec 2020

HAL is a multi-disciplinary open access archive for the deposit and dissemination of scientific research documents, whether they are published or not. The documents may come from teaching and research institutions in France or abroad, or from public or private research centers.

L'archive ouverte pluridisciplinaire **HAL**, est destinée au dépôt et à la diffusion de documents scientifiques de niveau recherche, publiés ou non, émanant des établissements d'enseignement et de recherche français ou étrangers, des laboratoires publics ou privés.

1
2 The far-infrared spectrum of ^{18}O enriched water vapour (40-700 cm^{-1})
3
4

5 S.N. Mikhailenko¹, S. Béguier², T.A. Odintsova³, M.Yu. Tretyakov³, O. Pirali^{4,5}, and A.
6 Campargue^{3,*}
7

8 ¹V.E. Zuev Institute of Atmospheric Optics, SB, Russian Academy of Science, 1, Academician Zuev square, 634055 Tomsk, Russia

9 ²Univ. Grenoble Alpes, CNRS, LIPhy, 38000 Grenoble, France

10 ³Institute of Applied Physics, Russian Academy of Sciences, Nizhniy Novgorod, Russia,

11 ⁴SOLEIL Synchrotron, L'Orme des Merisiers, Saint-Aubin 91192, Gif-Sur-Yvette, France

12 ⁵Université Paris-Saclay, CNRS, Institut des Sciences Moléculaires d'Orsay, 91405 Orsay, France
13
14
15
16
17
18
19
20
21
22
23
24
25
26
27
28
29
30
31
32
33
34
35
36

37 Key words: water vapour; far infrared; rotational spectrum; water isotope
38
39

40 * Corresponding author: Alain Campargue (alain.campargue@univ-grenoble-alpes.fr)
41

42 **Abstract**
43 The rotational spectrum of water vapour highly enriched in ¹⁸O has been studied by high resolution
44 ($\approx 0.001 \text{ cm}^{-1}$) Fourier transform spectroscopy at the AILES beam line of the SOLEIL synchrotron. The
45 room temperature absorption spectrum has been recorded between 40 and 700 cm^{-1} . The ¹⁸O enrichment of
46 the sample was about 97% while the gas pressure and the absorption pathlength were set to 0.97 mbar and
47 151.75 m, respectively. The spectrum contains more than 4800 rotational transitions from seven water
48 isotopologues (H_2^{18}O , H_2^{16}O , H_2^{17}O , HD^{18}O , HD^{16}O , HD^{17}O , D_2^{18}O). The assignments were performed
49 using known experimental energy levels as well as calculated line lists based on the results of Schwenke
50 and Partridge. The amount and accuracy of the reported line positions represent an important extension
51 compared to previous works. Overall, lines of about 2570 transitions are observed for the first time and 35,
52 41, 50, and 16 new energy levels are determined for H_2^{18}O , H_2^{17}O , HD^{18}O , and HD^{17}O , respectively. The
53 set of derived energy levels shows a number of important differences from those recommended by an
54 IUPAC-task group. Compared to the HITRAN2016 database, numerous deviations of line positions (up to
55 0.15 cm^{-1}) are found for the H_2^{17}O , H_2^{18}O , HD^{17}O , and HD^{18}O species. Incomplete and wrong HITRAN's
56 assignments of more than 90 transitions for H_2^{18}O , H_2^{17}O and HD^{18}O are identified. Overall, the measured
57 line positions will allow to significantly refine and complete the sets of empirical energy levels of H_2^{18}O ,
58 H_2^{17}O , HD^{18}O and HD^{17}O in the ground vibrational state.

59 **1. Introduction**

60 Water vapour plays a crucial role in the Earth's radiation budget determining our climate [1]. For
61 instance, the water distribution over the globe is permanently monitored by satellite based remote sensing
62 instruments [2]. In this context, a very accurate knowledge of water vapour absorption is required for a wide
63 variety of applications in geoscience [3]. This applies to the main isotopologue, H₂¹⁶O, but also to the less
64 abundant H₂¹⁸O, H₂¹⁷O and HD¹⁸O species (Note that only CO₂ is more abundant than H₂¹⁸O). Indeed,
65 quantitative information on the natural variation of isotopic abundance ratios, measured by absorption
66 methods, is currently used to trace various chemical and physical atmospheric processes (e.g. [4]). Note that
67 a complete and accurate line list of the water monomer, including line profile parameters, is also a
68 prerequisite for a reliable determination of the atmospheric continuum absorption, which is one of the oldest
69 and the long-standing problem in molecular spectroscopy (e.g., review papers [5-7] and references therein).

70 In the recent decades, new approaches to the calculation of vibration-rotation energy levels have been
71 developed up to the first dissociation limit (e.g. [8-11]). In general, theoretical line lists show important
72 advantages in terms of completeness, and quality of line intensity predictions. As concerns line positions,
73 theory does not yet compete with the experimental accuracy achieved using nowadays high resolution
74 spectrometers. As a result, recommended line lists for water vapour combine the advantages of experimental
75 and theoretical tools, calculated line positions being adjusted according to experimentally determined
76 energy levels. This method is that adopted for a large fraction of the water line list provided by the HITRAN
77 [12] and GEISA [13] databases.

78 The present work is devoted to an experimental study of the absorption spectrum of water vapour in
79 the far infrared region, below 700 cm⁻¹. It is commonly believed that the rotational transitions involving the
80 lowest vibrational states of light atmospheric molecules are sufficiently well known and characterized. The
81 results reported in this work indicate that a broad-band high resolution and high sensitivity recording of
82 water vapour spectrum in the far infrared range allows for a substantial extension of the previous knowledge
83 in the region. We believe that the main reason of the revealed information shortage in the THz and far-IR
84 spectral ranges (a region that we define as 1-15 THz or 30-500 cm⁻¹), is the insufficient performances of
85 laboratory spectrometers. While important technological progresses boosted the performances of
86 spectroscopic instruments in the microwave and IR domains in terms of frequency metrology, accessible
87 bandwidth, and sensitivity, the THz/far-IR lacks spectrometers allowing broadband surveys with MHz-level
88 spectral resolution. In the past decades, due to the atmospheric importance of water vapor, several (and often
89 unique) set-ups were applied to the far-IR spectroscopy of water vapor isotopologues [14-40]. They
90 provided valuable although incomplete set of observations with, in general, limited quality in terms of
91 accuracy and sensitivity. Fourier-Transform instruments, with improved spectral resolution over the years,
92 exploited the relatively weak far-IR continuum from global and/or mercury lamps to record absorption

93 spectra of water isotopologues [14-17, 19, 21, 33, 34, 38]. These recordings provided important survey data
94 but with limited frequency and intensity accuracy. In addition to absorption spectroscopy, the frequencies
95 of pure rotation transitions involving the ground and several excited vibrational states of H_2O could be
96 measured using various emission set-ups associated with FT interferometers [27-31, 37, 39, 40].

97 In order to improve the frequency accuracy of spectroscopic measurements in the far-IR, several
98 original instruments have been developed in few laboratories in late 90's. In particular, Evensons' type
99 tunable far-IR spectrometers [41], which principle is based on the mixing of two frequency stabilized CO_2
100 laser lines separated by few THz, allowed to record absorption spectra with few hundred kHz spectral
101 resolution. Using this instrumental approach, the Toyama University group was able to produce several
102 highly accurate line lists of water and its isotopologues in the 1-5 THz range [18, 24]. In a similar context,
103 Yu et al. [32] reported a combined analysis of highly accurate absorption spectra recorded with frequency
104 multiplication chains (up to 2.7 THz) together with a broadband far-IR FT emission spectra.

105 Recently, the advent of few beam lines extracting the far-IR radiation from synchrotron facilities
106 allowed recording Fourier transform far-IR spectra exhibiting much higher SNR than with the conventional
107 blackbody sources [23, 32, 42], despite a spectral resolution inherently limited to about 30 MHz for
108 commercial instruments. The increased sensitivity of these set-ups allowed the detection of relatively weak
109 signals as shown in our recent measurements of the far-IR water continuum absorption [43, 44], or the pure
110 rotation spectrum of O_2 [45]. In the present study, we used the experimental set-up developed on the AILES
111 beam line of synchrotron SOLEIL to extensively improve the far-IR dataset of water isotopic species
112 providing new frequency standards for these important molecules.

113 The paper is organized as follows. In Section II we present experimental details including the
114 spectrum acquisition and line list construction. The assignment of observed transitions is presented in
115 Section III. Comparison of our data with previously known information and closing remarks are given in
116 Section IV and V respectively.

117 **2. Experiment**

118 The Fourier-transform absorption spectrum of ^{18}O enriched water vapour was recorded in the 40 –
119 700 cm^{-1} region on the AILES beam line of SOLEIL synchrotron facility. The recordings were performed
120 during a measurement campaign devoted to the study of the far-infrared water vapour self-continuum
121 absorption [43, 44]. The continuum measurements were obtained using both water in natural isotopic
122 abundances and with a highly enriched ^{18}O sample (the impact of such isotopic substitution upon the water
123 self-continuum might give key insights on the physical nature of the water continuum). Note that the
124 continuum retrieval from the measured absorption requires the subtraction of the monomer contribution and
125 thus an accurate and complete line list of water monomer lines.

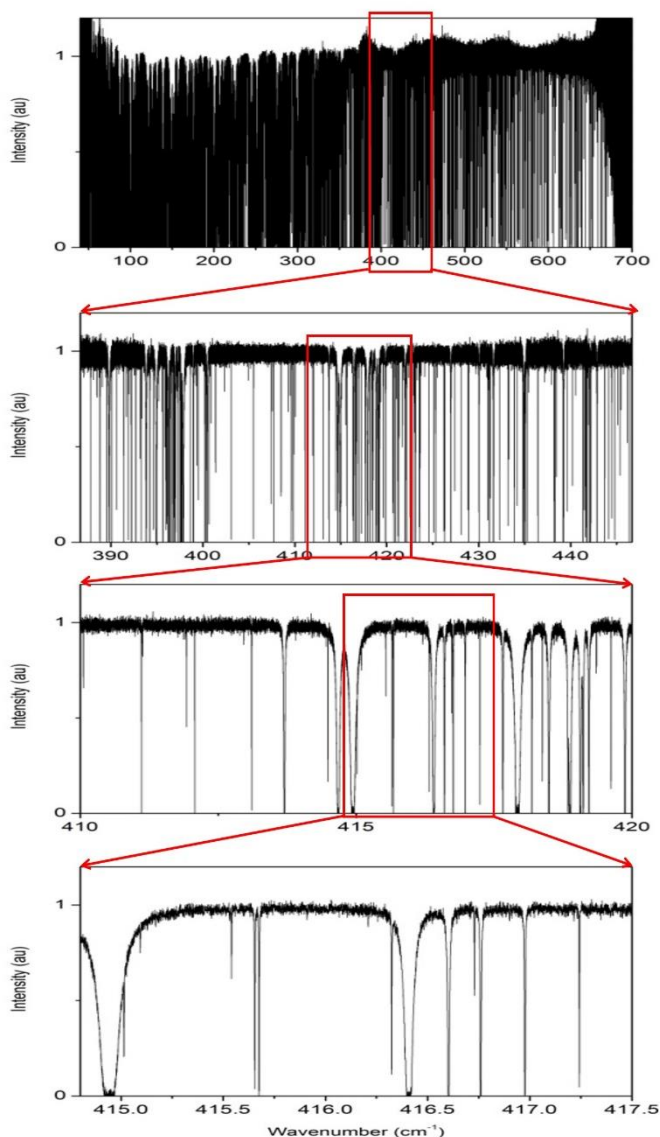


Fig. 1
 Successive zooms of the FTS spectrum of water vapour highly enriched in ^{18}O recorded at SOLEIL synchrotron at room temperature ($P=0.98$ mbar) between 40 and 700 cm^{-1} .

142 In the present work, the cell was filled with ^{18}O enriched water vapour (97% enrichment from
 143 Eurisotop) at a pressure of 0.98 mbar measured by a capacitance gauge (Pfeiffer 10 mbar full range with
 144 corresponding accuracy of 0.01 mbar). The resolution (defined as $0.9/\text{MOPD}$ where $\text{MOPD}=882$ cm is the
 145 maximum optical path difference) was set to 0.00102 cm^{-1} in Bruker' definition and no apodization of the
 146 interferogram was used (boxcar option of the Bruker software). The spectra were recorded in the 40-700
 147 cm^{-1} spectral range using the SOLEIL synchrotron radiation in standard mode, together with a 4 K cooled
 148 Si bolometer detector and the 6 μm mylar-composite beam splitter. The absorption spectra were obtained
 149 using a multipass cell in White-type configuration. The total absorption path length was set to 151.75 ± 1.5
 150 m corresponding to 60 passes between mirrors separated by 2.52 m and about 0.5 m of space between the
 151 50 μm thick polypropylene films windows. The spectrum was recorded at room temperature (298.0(3) K),

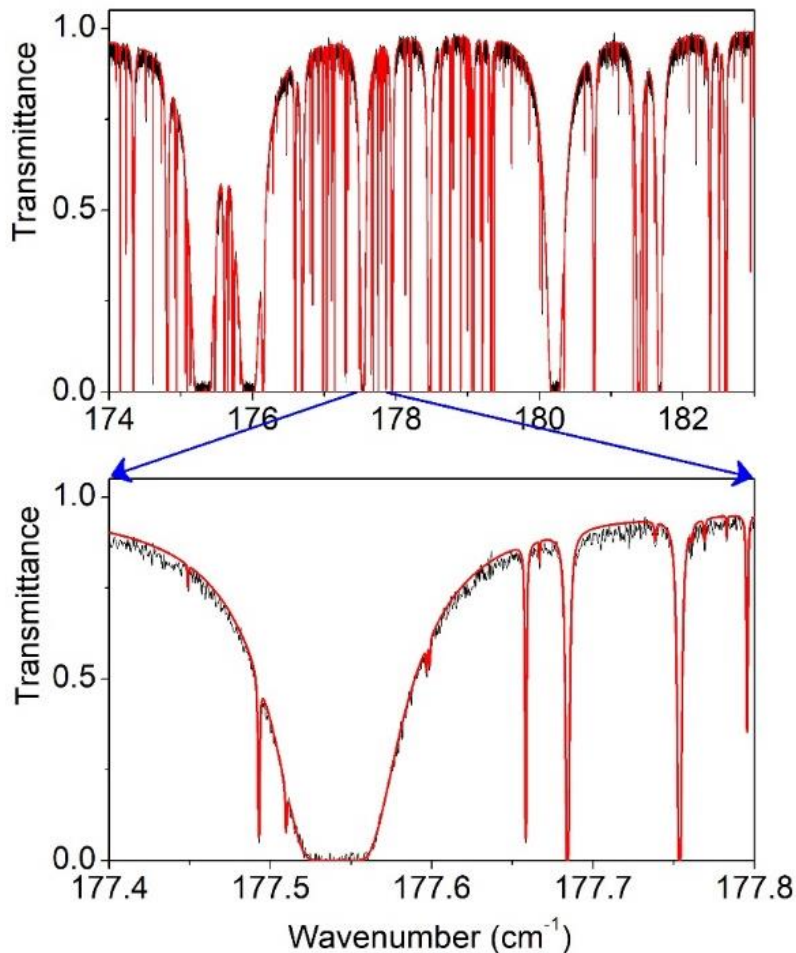
152 that was monitored by a pair of platinum sensors mounted on the cell external surface. Two hundred spectra
153 corresponding to a recording time of 10 hours were co-added. An overview of the transmittance spectrum
154 is displayed on the upper panel of **Fig. 1**, which include successive zooms. The absorption coefficient was
155 determined as $\alpha_{total} = 1/L \ln(I_0(\nu)/I(\nu))$, where $I(\nu)$ and $I_0(\nu)$ correspond to the spectrum with the cell
156 filled with water vapour and evacuated, respectively.

157 The absolute frequency calibration was performed by frequency matching of 380 measured line
158 centers of intermediate intensities with accurate H_2^{16}O line positions from Refs. [17-19, 23, 24, 26, 32]. As
159 a result of the calibration procedure, the statistical uncertainty of the line centers is estimated to increase
160 from $3 \times 10^{-5} \text{ cm}^{-1}$ to $1 \times 10^{-4} \text{ cm}^{-1}$ over the 50-700 cm^{-1} range of the recordings. Note that, at the recording
161 pressure of 0.98 mbar, the amplitude of the water line pressure shifts may reach $0.1 \text{ cm}^{-1}/\text{atm}$ for lowest $J =$
162 0 and 1 transitions. For these lines we recommend increasing the evaluated uncertainty up to $2 \times 10^{-4} \text{ cm}^{-1}$
163 until accurate data on line shift coefficients become available. For larger J values, the shift magnitude
164 decreases and thus a total uncertainty of $1 \times 10^{-4} \text{ cm}^{-1}$ is believed to be a conservative estimate.

165 The line parameters retrieval was performed using a homemade multiline fitting program in
166 LabVIEW and C++. In our pressure conditions, the pressure broadening (about $4 \times 10^{-4} \text{ cm}^{-1}$ HWHM at 1
167 mbar [12]), the Doppler broadening (on the order of $1.5 \times 10^{-4} \text{ cm}^{-1}$ near 100 cm^{-1}) and the apparatus function
168 (about $3.5 \times 10^{-4} \text{ cm}^{-1}$ HWHM) contribute significantly to the line profile. The present study being mainly
169 focused on line positions, the FTS transmittance spectrum was fitted assuming the standard Voigt line
170 profile as line shape. As starting point of the fit, an empirical line list including line profile parameters was
171 prepared mainly on the basis of the HITRAN database [12], intensity values being scaled according to
172 estimated values of the isotopic abundances. The water isotopologue identification included in this
173 preliminary list was used to fix the Doppler broadening according to the mass of the involved isotopologue.
174 We intended to adjust the position, area and Lorentzian width of the different lines but in the case of strongly
175 “saturated” lines, due to the high opacity, the line profile parameters were generally constrained to their
176 default values and only the position and area were fitted. **Fig. 2** illustrates the achieved spectrum
177 reproduction. In the case of lines of intermediate intensity, residuals (obs. – calc.) corresponding to the noise
178 level ($\sim 2\%$ of the empty cell transmittance) was generally achieved. This value corresponds to a noise
179 equivalent absorption on the order of 10^{-6} cm^{-1} and a detectivity threshold of about $10^{-25} \text{ cm}/\text{molecule}$ for
180 the line intensities.

181 Overall, line parameters of 5262 absorption features were retrieved. This large dataset includes about
182 1000 “saturated” water lines too strong to be accurately measured in our experimental conditions. Indeed,
183 the investigated spectral region involves very strong transitions with intensity larger than $10^{-18} \text{ cm}/\text{molecule}$
184 while the pressure and absorption pathlength conditions of the studied spectrum are suitable for derivation
185 of line intensities in the $5 \times 10^{-25} - 8 \times 10^{-23} \text{ cm}/\text{molecule}$ range (see below).

186



187

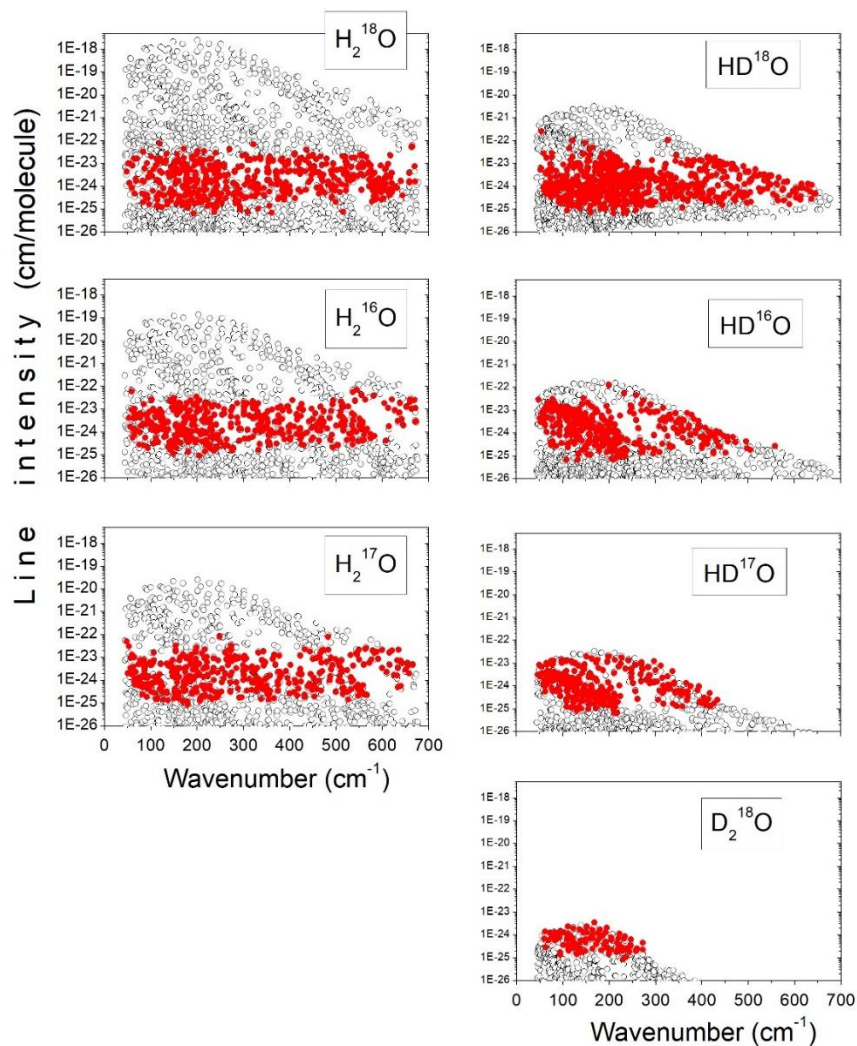
188 **Fig. 2**

189 Comparison of the FTS spectrum of water vapour highly enriched in ^{18}O near 175 cm^{-1} to a simulation using
 190 a Voigt profile as line shape.

191

192 3. Rovibrational assignments

193 The rovibrational assignments were performed using literature results as well as calculated line lists
 194 based on the results of Schwenke and Partridge (SP) [8, 9]. 4610 lines were assigned to 4824 transitions
 195 (some absorption features correspond to several transitions) of seven water isotopologues (see **Table 1**). In
 196 addition, on the basis of the HITRAN2016 database [12], 100 lines were assigned to transitions of HF, NH_3 ,
 197 $^{12}\text{C}^{16}\text{O}_2$, and $^{12}\text{C}^{18}\text{O}_2$ present as impurities in the sample, with estimated relative concentration of 1, 2, 10
 198 and 7 ppm (Note the strong ^{18}O enrichment of CO_2 probably due to oxygen atom exchanges between ^{18}O
 199 enriched water vapor and natural carbon dioxide). 552 lines with intensity below $8.3 \times 10^{-25}\text{ cm/molecule}$
 200 remain unassigned. The relative abundances of the different water isotopologues were estimated from the
 201 ratio of the measured line intensities to their calculated values [46-51].



202 **Fig. 3**
 203 Overview of the presently assigned transitions for the different water isotopologues between 44 and 678
 204 cm^{-1} . The plotted observations (red points) are limited to “unsaturated” lines for which line parameters could
 205 be reliably determined. Open circles correspond to the HITRAN2016 line list except for D_2^{18}O , absent in
 206 the HITRAN database, for which the predictions based on Schwenke and Partridge calculations [8, 9] were
 207 used.
 208
 209

210 **Fig. 3** shows an overview of the “unsaturated” assigned lines for the different isotopologues. The
 211 number of assigned transitions, maximum values of rotational numbers and spectral range are given in **Table**
 212 **1**. The number of newly observed transitions included in the table indicates that new transitions are observed
 213 for the seven isotopologues, in particular the main one, H_2^{16}O , although its relative abundance was limited
 214 to about 5% in the used water sample. For the H_2^{18}O molecule, the observed lines are rotational transitions
 215 within the ground vibrational state or within the (010) and (020) bending states (vibrational states are
 216 labelled $(\nu_1\nu_2\nu_3)$ where ν_1, ν_2, ν_3 are the quantum numbers corresponding to the symmetric stretch, bending
 217 and antisymmetric stretch, respectively). For the H_2^{16}O , H_2^{17}O , HD^{16}O and HD^{18}O isotopologues, only

218 rotational transitions within the (000) and (010) states are detected while for the least abundant HD ^{17}O and
 219 D $_2^{18}\text{O}$ species, only ground state rotational transitions were assigned.

220 **Table 1.** Line-by-line statistics of water transitions assigned between 44 and 678 cm $^{-1}$

Molecule	Abundance	NT^a	NT_{new}^b	J_{\max}	$K_{a\max}$	Range, cm $^{-1}$
H $_2^{16}\text{O}$	0.0523	816	37	19	12	44.099 – 673.284
H $_2^{18}\text{O}$	0.9345	1206	762	21	14	44.218 – 677.744
H $_2^{17}\text{O}$	9.4×10^{-3}	675	318	18	12	44.218 – 665.558
HD ^{16}O	2.06×10^{-4}	528	133	18	10	46.206 – 558.092
HD ^{18}O	3.51×10^{-3}	1126	926	21	12	44.866 – 645.736
HD ^{17}O	3.72×10^{-5}	363	324	16	10	46.023 – 433.483
D $_2^{18}\text{O}$	3.75×10^{-6}	110	38	15	10	59.554 – 271.653
Total		4824	2538	21	14	44.099 – 677.744

221 *Notes*

222 aNT – Number of transitions contributing to the spectrum (including “saturated” lines too strong to be accurately
 223 measured)

224 $^bNT_{new}$ – Number of transitions which were previously unobserved in absorption or in emission.
 225

226 We provide as supplementary material the fitted parameter values of 3625 lines, which could be
 227 reliably determined, thus excluding many “saturated” lines. The position comparison presented below
 228 applies to this set of transitions.

229 Following the exhaustive review of the literature presented in the next paragraph, 35, 41, 50, and 16
 230 new energy levels are determined for H $_2^{18}\text{O}$, H $_2^{17}\text{O}$, HD ^{18}O , and HD ^{17}O , respectively. They are listed in

231 **Table 2.**

J	K_a	K_c	Energy ^a	δE^b
HD¹⁷O				
8	7	2	1286.95798	24
8	7	1	1286.95806	25
9	5	4	1077.48245	16
9	6	4	1237.64510	21
11	2	9	1137.95227	23
11	4	8	1273.25513	17
11	4	7	1282.27792	22
12	3	9	1400.64291	32
12	4	8	1476.06777	27
13	4	9	1687.62496	42
15	0	15	1623.95330	60
15	1	15	1623.95890	51
15	1	14	1807.63052	55
15	2	14	1807.86174	57
16	0	16	1832.90619	56
16	1	16	1832.90869	56
HD¹⁸O				
11	11	1	2727.92355	17
11	11	0	2727.92356	17
12	10	3	2625.80073	10
12	10	2	2625.80071	11
12	11	2	2907.45459	17
12	11	1	2907.45459	16
12	12	1	3211.69276	20
12	12	0	3211.69275	20
13	10	4	2821.45430	11
13	10	3	2821.45437	11
13	11	3	3101.84662	15
13	11	2	3101.84664	15
13	12	2	3404.72928	20
13	12	1	3404.72928	20
14	9	6	2776.11040	10
14	9	5	2776.11032	11
14	10	5	3032.03855	13
14	10	4	3032.03955	13

14	11	4	3311.06726	15
14	11	3	3311.06719	15
15	6	9	2390.77152	7
15	7	8	2567.59499	8
15	8	8	2772.56672	10
15	8	7	2772.56729	16
15	9	7	3003.01555	13
15	9	6	3003.01461	10
15	10	6	3257.51792	15
15	10	5	3257.51800	14
16	6	10	2639.47084	9
16	7	9	2813.03401	13
16	8	9	3016.06013	12
16	8	8	3016.07130	14
16	9	8	3244.89230	20
16	9	7	3244.90173	15
17	4	13	2691.62971	11
17	5	13	2746.38188	14
17	5	12	2779.97472	13
17	6	11	2904.61371	12
17	7	10	3073.91144	15
18	4	15	2868.61008	14
19	1	18	2759.48253	17
19	2	18	2759.49883	21
19	2	17	2967.05298	17
19	3	17	2967.43987	20
20	0	20	2782.54227	23
20	1	20	2782.54232	23
20	1	19	3029.29136	24
20	2	19	3029.29996	20
21	0	21	3051.90805	26
21	1	21	3051.90800	26
H₂¹⁷O				
12	11	2	3493.27691	64
12	11	1	3493.27731	66
12	12	1	3744.31027	75
12	12	0	3744.31067	73

13	7	7	2918.03362	46
13	8	6	3116.43172	54
13	9	5	3333.91518	58
13	9	4	3333.91904	44
13	10	4	3566.86888	63
13	10	3	3566.86799	50
13	11	3	3811.88536	71
13	11	2	3811.88481	65
14	4	10	2876.88740	34
14	5	10	2912.22127	44
14	5	9	2979.51743	41
14	6	9	3077.62393	51
14	6	8	3095.29248	40
14	7	8	3255.17281	46
14	7	7	3257.54686	45
14	8	7	3453.37869	51
14	9	6	3671.37911	60
15	1	14	2625.42191	48
15	2	14	2625.43495	51
15	2	13	2866.13932	46
15	3	13	2866.41578	47
15	3	12	3074.19168	49
15	4	11	3239.69214	51
15	6	9	3467.06349	51
15	7	8	3620.21357	64
16	1	15	2945.81632	65
16	2	15	2945.82275	61
16	3	14	3204.28827	61
16	4	13	3432.23621	59
17	0	17	2974.64780	77
17	1	17	2974.65177	89
17	1	16	3283.81730	76
17	2	16	3283.82057	74
17	2	15	3559.46121	71
18	0	18	3311.98363	97
18	1	18	3311.97966	86
18	2	17	3639.33094	84

H₂¹⁸O				
15	5	11	3257.12317	8
16	1	15	2939.95141	10
16	3	13	3424.23366	11
16	4	12	3612.34609	11
16	5	11	3749.54756	12
16	6	10	3859.76914	10
16	8	8	4185.60745	13
17	2	16	3277.27565	12
17	2	15	3552.56928	9
17	3	15	3552.63498	12
17	3	14	3796.19838	9
17	4	14	3797.10678	14
17	5	13	4012.43988	12
18	0	18	3305.31389	13
18	1	18	3305.31308	11
18	1	17	3632.07157	13
18	2	17	3632.07254	11
18	2	16	3924.35214	13
18	3	16	3924.38536	11
18	3	15	4184.79228	16
18	4	15	4185.28138	11
18	5	14	4416.22560	11
18	15	3	6806.97939	120
19	0	19	3659.47265	13
19	1	19	3659.47360	15
19	1	18	4004.24664	13
19	2	18	4004.24772	15
19	2	17	4313.21925	12
19	3	17	4313.23774	15
20	0	20	4031.03352	17
20	1	20	4031.03257	16
20	1	19	4393.69352	17
20	2	19	4393.69394	14
21	0	21	4419.88437	17
21	1	21	4419.88532	19

234

Table 2. New energy levels of H₂¹⁸O, H₂¹⁷O, HD¹⁸O, and HD¹⁷O determined from the analysis of the FTS spectrum of water vapour highly enriched in ¹⁸O between 44 and 678 cm⁻¹.

Notes

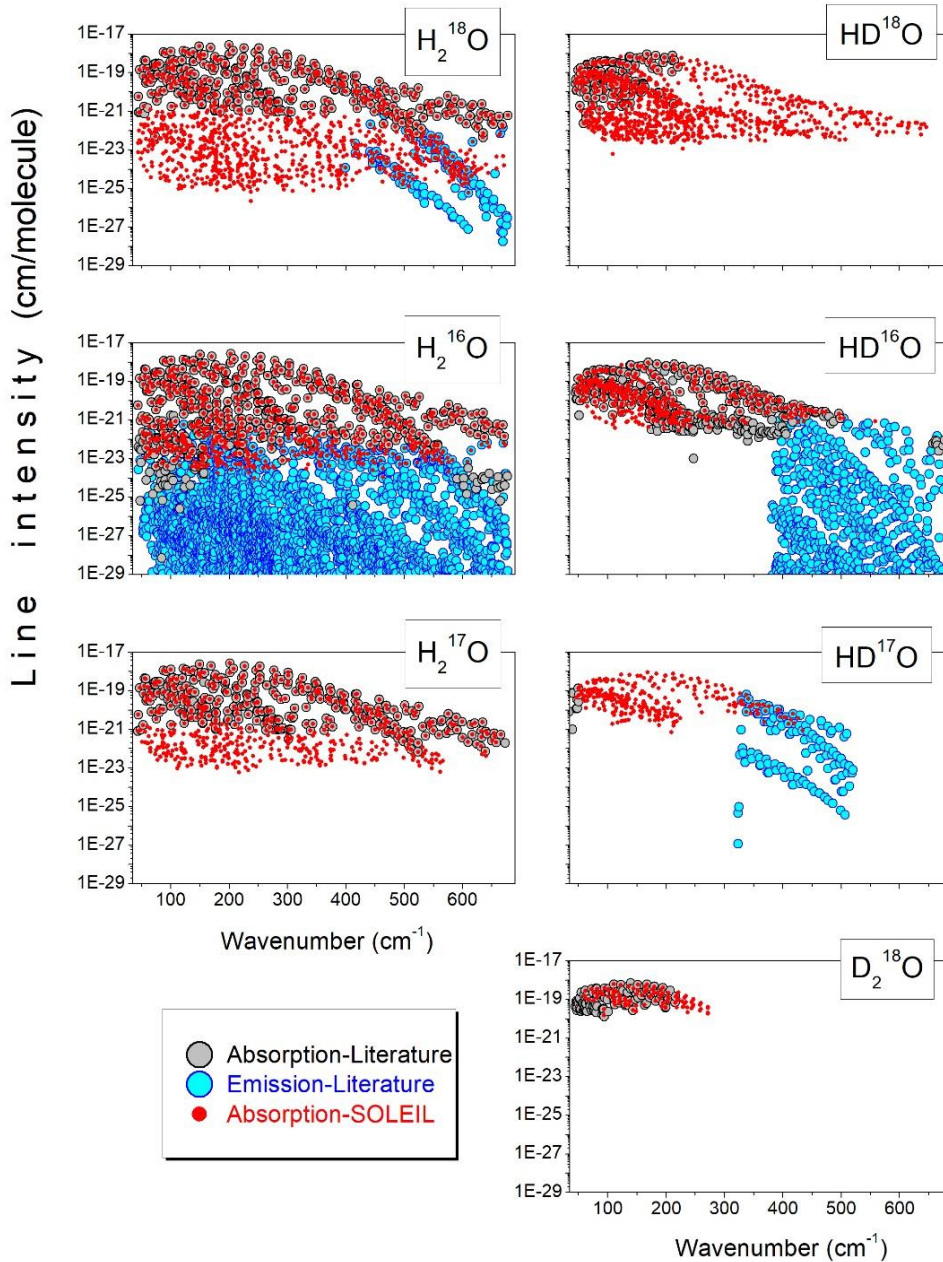
^a Term energy in cm⁻¹

^b Statistical uncertainty in 10⁻⁵ cm⁻¹

240 **4. Comparison to literature**

241 *4.1. Previous experimental studies*

242 Some years ago, an IUPAC task group performed an exhaustive review of the experimental
243 investigations of the absorption and emission spectra of the various water isotopologues [52-55]. Each of
244 the IUPAC-TG report includes a table listing the studies available at that time and for each work, the spectral
245 range, the number of reported transitions and the main experimental characteristics. Most of the available
246 experimental data in our region of interest have been obtained by FTS. In particular, several FTS emission
247 spectra provided a considerable amount of observations which should be used with caution because emission
248 line positions are in general less accurate as they suffer from frequent line overlapping and significant
249 Doppler broadening in the case of hot spectra. Overall, most of the previous absorption studies are not recent
250 and limited to less than one hundred lines. This is due to the fact that, all literature works but Ref. [36], used
251 natural water or a moderated isotopic enrichment in ^{18}O while a water vapour highly enriched in H_2^{18}O and
252 a long absorption pathlength are presently used. The large amount of newly measured transitions is
253 illustrated in **Fig. 4** where previous observations by absorption and emission spectroscopy are distinguished.
254 In order to give an overview of the available transition wavenumbers, we have associated a line intensity
255 (HITRAN values scaled to 100% abundance for each isotopologue) to all the wavenumbers reported in the
256 literature both in absorption and in emission. Compared to previous absorption studies, a considerable gain
257 is noted for all the isotopologues but H_2^{16}O and HD^{16}O . In particular, the present measurements lower from
258 10^{-21} to 10^{-25} cm/molecule, the detectivity threshold of H_2^{18}O lines and a gain of two orders of magnitude is
259 noted for H_2^{17}O and HD^{18}O . Previous HD^{17}O measurements were practically absent in this spectral region.



260
 261 **Fig. 4**
 262 Overview comparison of the present observations (red points) to previous literature data. Transitions from
 263 the literature observed by absorption and emission spectroscopy are indicated by grey and blue circles,
 264 respectively. For the sake of the comparison, we have affected an absorption line intensity to the emission
 265 data. Line intensities correspond to the pure species (100 % abundance).
 266

267 Below we give a brief updated summary of the present knowledge for the various isotopologues in
 268 the region of interest (44-678 cm^{-1}).

269 The most extensive study of H_2^{16}O absorption lines in the region was reported by Kauppinen et al.
 270 [14] in 1978. 382 pure rotational transitions and 17 transitions of the ν_2 - ν_2 band were reported. Later,

271 additional 233 rotational transitions in absorption were reported in Refs. [15-25]. Besides, hot emission
272 spectra provided a high number of rotational and rotation-vibration transitions in the ground and 15 excited
273 vibrational states [26-32]. Overall, 2868 different rotational transitions were reported in Refs. [14-32] within
274 the ground and first excited ($v_2=1$) vibrational states.

275 H_2^{18}O and H_2^{17}O

276 The literature data concerning these minor isotopologues is limited. In 1977, Winther measured 121
277 and 48 pure rotational transitions of H_2^{18}O and H_2^{17}O , respectively, by absorption FTS in natural water
278 vapour below 501 cm^{-1} [33]. Later, 255 absorption transitions were reported for H_2^{18}O in Refs. [14, 15, 17,
279 21, 34-36]. Note that only one transition ($3_{22} - 3_{13}$ at 73.31376 cm^{-1}) was reported by Johns [17] for the
280 first excited state ($v_2=1$). Finally, Mikhailenko et al. [37] assigned 127 H_2^{18}O emission lines to 144
281 transitions in the $399 - 677\text{ cm}^{-1}$ region. 36 of these 144 transitions belong to the v_2-v_2 band. Overall, 498
282 rotational absorption and emission transitions in the (000) and (010) states were reported in Refs. [14, 15,
283 17, 21, 33-37] for H_2^{18}O . As for H_2^{17}O , all the 364 transitions known in the far-IR range are pure rotational
284 transitions [14, 15, 17, 21, 33-36].

285 HD^{16}O

286 Only four high resolution studies of HD^{16}O absorption were reported in the studied frequency range.
287 Sixty pure rotational transitions were reported in 1978 by Kauppinen et al. [14] between 152 and 419 cm^{-1} .
288 Later, Johns [17], Paso & Horneman [19] and Toth [38] expanded the studied range to $45 - 677\text{ cm}^{-1}$ leading
289 to a total number of 528 transitions. More recently, Janca et al. reported the HD^{16}O emission spectrum above
290 381 cm^{-1} [39]. Overall, 1168 transitions within the ground and $v_2=1$ vibrational states were reported in our
291 region in Refs. [14, 17, 19, 38, 39].

292 HD^{18}O and D_2^{18}O

293 182 and 136 pure rotational transitions between 44 and 220 cm^{-1} were reported by Johns [17] for
294 HD^{18}O and D_2^{18}O , respectively. More recently, Yu et al. [56] reported accurate measurements of 31
295 transitions between 50 and 134 cm^{-1} for HD^{18}O .

296 HD^{17}O

297 Up to now, only six transitions of HD^{17}O were measured in absorption [57]. They are located between
298 46.0 and 50.4 cm^{-1} and show a resolved hyperfine structure due to the nuclear spin of ^{17}O . In a recent FTS
299 emission study, Mellau et al. [40] assigned 189 transitions to 169 emission lines between 320 and 520
300 cm^{-1} . These measurements provided an extended set of the energy levels of the ground and first excited
301 ($v_2=1$) states up to $J_{max} = 17$ and $K_{a\ max} = 13$.

302 4.2. HITRAN database

303 **Table 3** summarizes the contents of the HITRAN2016 water line list [12] in the 44 - 678 cm^{-1} region.
304 21768 transitions of seven isotopologues H_2^{16}O , H_2^{18}O , H_2^{17}O , HD^{16}O , HD^{18}O , HD^{17}O , and D_2^{16}O in natural

305 abundance are listed with intensity cut-offs ranging between 2.3×10^{-34} and 2.0×10^{-31} cm/molecule depending
 306 on the species. The last column of the table gives the source of the HITRAN2016 line positions and line
 307 intensities. For all but the main isotopologue, line intensities are *ab initio* values while line positions were
 308 calculated from IUPAC-TG energy levels when available or, otherwise, from *ab initio* energy levels. In the
 309 case of H_2^{16}O , 2507 rotation and rotation-vibration transitions in the five lowest vibration states - (000),
 310 (010), (020), (100), and (001) - originate from an effective operator approach [46, 49, 58, 59]. For transitions
 311 involving other vibrational states, HITRAN line parameters were obtained in the same way as for the minor
 312 isotopologues (see Section 2.1 of Ref. [12]).

313 **Table 3.** HITRAN2016 water contents between 44 and 678 cm^{-1}

Isotopologue	Abundance	Number of transitions	Intensity cut-off (cm/molecule)	References	
				Position	Intensity
H_2^{16}O	0.997317	6551	1.026×10^{-32}	[54, 58, 59]	[46-49]
H_2^{18}O	0.00199983	2261	1.350×10^{-31}	[52, 60, 61]	[50]
H_2^{17}O	0.000371884	1832	2.020×10^{-31}	[50, 61]	[50]
HD^{16}O	0.000310693	4363	1.473×10^{-31}	[51]	[51]
HD^{18}O	0.000000623003	1824	1.500×10^{-31}	[51, 62]	[51]
HD^{17}O	0.000000115853	1403	1.576×10^{-31}	[51, 62]	[51]
D_2^{16}O	0.000000024197	3534	2.301×10^{-34}	[51, 62]	[51]
Total		21,768	2.301×10^{-34}		

314 The systematic comparison of our observation to HITRAN line list revealed that six high rotational
 315 transitions of H_2^{18}O with $J > 17$ observed in our spectrum are missing in the HITRAN list. Ninety-two
 316 rotational transitions of H_2^{18}O , H_2^{17}O and HD^{18}O are provided with incomplete or erroneous assignments.
 317 The list of H_2^{18}O missing lines and the corrected assignments are provided as Supplementary Material.
 318

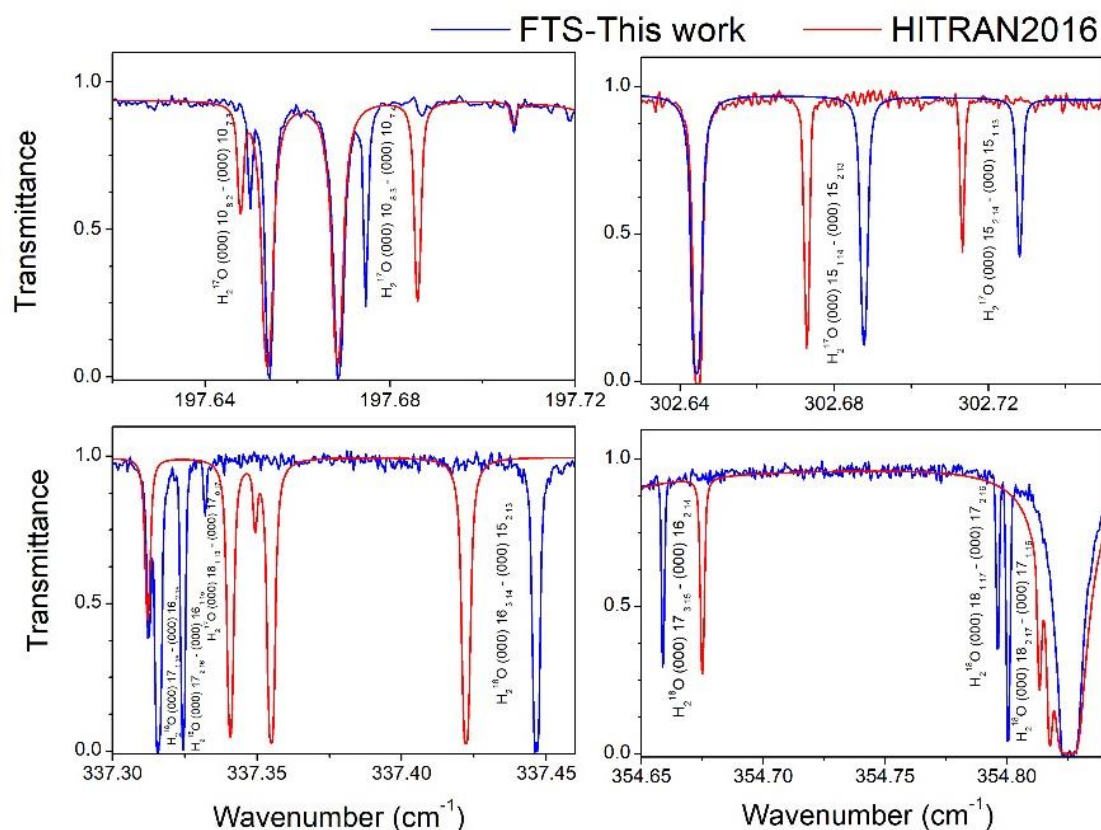
319 **Table 4.** Line position comparison with HITRAN2016 [12]

Molecule	NT^a	δv_{max} (10^{-3} cm^{-1})	δv (10^{-3} cm^{-1}) ^b			
			$\delta v < 0.1$	$0.1 \leq \delta v < 0.5$	$0.5 \leq \delta v < 1.0$	$\delta v \geq 1.0$
H_2^{16}O	604	0.57	399	201	4	
H_2^{18}O	734	43.96	191	295	103	145
H_2^{17}O	619	35.51	241	202	52	124
HD^{16}O	504	3.04	275	211	14	4
HD^{18}O	984	152.54	411	369	101	103
HD^{17}O	356	117.21	43	180	66	67
Total	3801	152.54	1560	1458	340	546

320
 321 *Notes*

322 ^a NT – number of transitions

323 ^b Absolute value of the ($v_{\text{meas.}} - v_{\text{IUPAC}}$) position difference in 10^{-3} cm^{-1} unit.

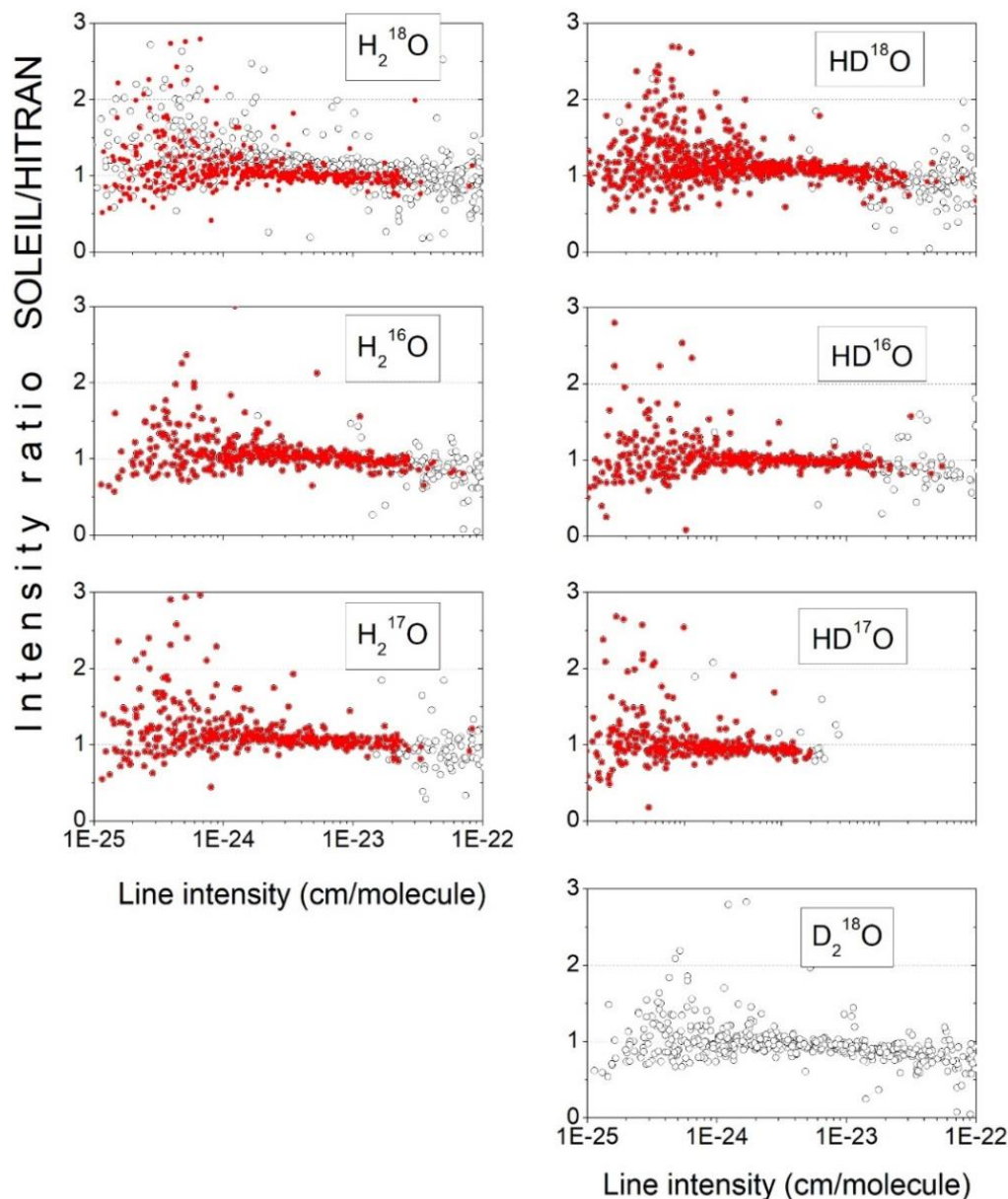


324
 325 **Fig. 5**
 326 Comparison of the recorded spectrum to a simulation based on the HITRAN2016 database in the same
 327 experimental conditions.

328
 329 **Table 4** summarizes the results of the systematic comparison of our measured line positions to
 330 HITRAN values. The comparison applies to lines “unsaturated” in our spectrum (see **Fig. 3**). Due to an
 331 extremely small natural relative abundance, D_2^{18}O transitions are not included in the HITRAN list. **Table 4**
 332 gives the number of transitions corresponding to different ranges of deviations. Overall, a very good
 333 agreement is observed for H_2^{16}O and to a less extent for HD^{16}O . This is not the case for the H_2^{18}O , H_2^{17}O ,
 334 HD^{18}O and HD^{17}O species which show a significant fraction of positions deviating by more than 10^{-3} cm^{-1} .
 335 Maximum deviations correspond to *ab initio* values from Refs. [50, 51] and exceed 0.03 cm^{-1} for H_2^{18}O and
 336 H_2^{17}O and 0.11 cm^{-1} for HD^{18}O and HD^{17}O . **Fig. 5** shows a comparison of our FTS spectrum to an HITRAN
 337 simulation in the experimental conditions of the recordings in several spectra intervals where HITRAN data
 338 deviate importantly from the observations.

339 The ratios of measured and HITRAN line intensities were used to determine the isotopologue
 340 abundance in our sample except for the D_2^{18}O , absent in the HITRAN list, for which the calculated SP
 341 intensities [8,9] were used. The obtained ratios are plotted in **Fig. 6** versus the measured line intensities. In

342 order to get an average intensity ratio of unity, the reference intensity values (HITRAN or SP) were scaled
 343 according to the abundance values given in **Table 1**. The more reliable sets of ratios corresponding to
 344 “unsaturated” lines are highlighted. Overall, the achieved agreement is reasonable. Large errors in the
 345 retrieval of the line intensities are believed to be responsible of the observed outliers.



346
 347 **Fig. 6**
 348 Ratios of measured and HITRAN line intensities *versus* experimental intensity values (for D_2^{18}O , SP
 349 calculated values [8, 9] are used instead of HITRAN values [12]). The average intensity ratio was fixed
 350 close to unity, by scaling the HITRAN (or SP) intensity values according to the abundance values given in
 351 Table 1. The more reliable ratios corresponding to “unsaturated” lines are highlighted (red dots).
 352

353 4.3. IUPAC Task group

354 The energy levels recommended by the IUPAC-TG [52-55] have been used to calculate the line
 355 centers of our measured transitions. The comparison (**Table 5**) applies to the same set of unsaturated lines
 356 as for the HITRAN comparison (**Table 4**). Similarly to the HITRAN comparison, **Table 5** gives the number
 357 of transitions corresponding to different ranges of deviations. The considered observed transitions of H_2^{18}O ,
 358 H_2^{17}O , HD^{18}O , and HD^{17}O involve 503, 329, 415 and 187 energy levels, respectively. For these four species,
 359 the maximum position differences are on the order of 0.03 cm^{-1} and a total of 543 IUPAC positions could
 360 not be calculated because they involve levels absent in the IUPAC-TG datasets. More than 10% of the
 361 compared line positions deviate by more than 10^{-3} cm^{-1} *i.e.* by more than ten times the accuracy of our
 362 reported line positions, suggesting that the IUPAC values of the involved energy levels should be
 363 significantly corrected. Note that for HD^{18}O , we excluded from **Table 5**, the largest position difference
 364 corresponding to the $14_{3\ 11} - 13_{2\ 12}$ transition ($\nu_{\text{OBS}} = 438.44685\text{ cm}^{-1}$ while $\nu_{\text{IUPAC}} = 195.91293\text{ cm}^{-1}$). This
 365 error is due to the fact that the upper energy level at 1592.7268 cm^{-1} in the IUPAC energy data set [53] is
 366 assigned to the (000) $14_{3\ 11}$ level and not to the level (000) $14_{1\ 13}$. In fact, this is a result of erroneous
 367 assignments of three ν_3 transitions in Ref. [63]. The transitions at 3457.1689 , 3482.6769 , 3483.1638 cm^{-1}
 368 assigned in Ref. [63] as $13_{1\ 12} - 14_{1\ 13}$, $13_{3\ 10} - 14_{3\ 11}$ and $13_{2\ 12} - 14_{3\ 11}$, respectively, should be assigned
 369 to $13_{3\ 10} - 14_{3\ 11}$, $13_{1\ 12} - 14_{1\ 13}$ and $13_{2\ 12} - 14_{1\ 13}$, respectively.

370

371 **Table 5.** Line position comparison with values calculated using the IUPAC-TG energy levels

372

Molecule	NT^a	NTO^b	$\delta\nu_{\text{max}}$ (10^{-3} cm^{-1})	$\delta\nu$ (10^{-3} cm^{-1}) ^d			
				$\delta\nu < 0.1$	$0.1 \leq \delta\nu < 0.5$	$0.5 \leq \delta\nu < 1.0$	$\delta\nu \geq 1.0$
H_2^{16}O	604	0	7.43	208	286	76	34
H_2^{18}O	734	43	39.61	189	294	102	106
H_2^{17}O	619	49	34.98	248	202	49	71
HD^{16}O	504	0	1.06	275	212	13	4
HD^{18}O	984	277	29.61 ^c	105	284	131	187
HD^{17}O	356	174	36.24	45	81	30	26
D_2^{18}O	110	0	2.83	31	63	7	9
Total	3911	543	39.61 ^{c)}	1101	1422	408	437

373

374

Notes

375

^a NT – number of transitions

376

^b NTO – number of transitions that could not be calculated for IUPAC energy levels [52, 53]

377

^c Excluding the $14_{3\ 11} - 13_{2\ 12}$ pure rotation transition ($\nu_{\text{OBS}} = 438.44685\text{ cm}^{-1}$ while $\nu_{\text{IUPAC}} = 195.91293\text{ cm}^{-1}$ (see Text).

378

379

^d Absolute value of the ($\nu_{\text{OBS}} - \nu_{\text{IUPAC}}$) position difference in 10^{-3} cm^{-1} unit.

380

381 **5. Concluding remarks**

382 The knowledge of the absorption spectrum of water vapour, in particular of the minor isotopologues,
383 has been significantly improved in the range of the rotational band, on the basis of a FTS spectrum highly
384 enriched in ¹⁸O recorded at the AILES beam line of the SOLEIL synchrotron. The quality of the recorded
385 high resolution spectrum benefitted from the high photon flux and large spectral coverage provided by the
386 synchrotron source. The use of a 151.75-m absorption pathlength allows for the detection of 2538 new
387 transitions of seven water isotopologues (H₂¹⁸O, H₂¹⁶O, H₂¹⁷O, HD¹⁸O, HD¹⁶O, HD¹⁷O, D₂¹⁸O). Overall,
388 one hundred and forty-two energy levels were newly determined for H₂¹⁸O, H₂¹⁷O, HD¹⁸O, and HD¹⁷O. In
389 addition, for a large fraction of previously measured transitions (in particular those derived from emission
390 spectra), the line position accuracy (about 10⁻⁴ cm⁻¹) is significantly improved. The systematic comparison
391 to the HITRAN2016 database and to the position values derived from the IUPAC-task energy levels reveals
392 a significant number of inaccuracies. Considering that the observed transitions involve the lowest vibrational
393 states of most of the water vapour transitions, the energy levels corrections evidenced in the present study
394 will propagate to a large number of energy values of excited vibrational levels.

395
396 **Acknowledgements**

397 This work became possible due to the Project No 20180347 supported by SOLEIL Synchrotron Team.
398 TAO and MYT acknowledge the support from the joint RFBR-CNRS project No 18-55-16006. SNM
399 activity was supported by the Ministry of Science and Higher Education of the Russian Federation (Project
400 No. AAAA-A17-117021310147-0). The support of the CNRS (France) in the frame of International
401 Research Project SAMIA is acknowledged.

402

References

- 403 1. Wayne RP. Chemistry of atmospheres. New York: Oxford University Press; 3rd edn., 2000.
- 404 2. Schröder M, Lockhoff M, Shi L, August T, Bennartz R, Borbas E, et al. 2017: GEWEX water vapor
405 assessment (G-VAP). WCRP Report 16/2017; World Climate Research Programme (WCRP): Geneva,
406 Switzerland; 216 pp. ([https://www.wcrp-climate.org/WCRP-publications/2017/WCRP-Report-16-
407 2017-GVAP-v1.3_web.pdf](https://www.wcrp-climate.org/WCRP-publications/2017/WCRP-Report-16-2017-GVAP-v1.3_web.pdf) See Section 3, p.26)
- 408 3. Bernath PF. The spectroscopy of water vapour: Experiment, theory and applications. Phys Chem Chem
409 Phys 2002;4:1501-9. <https://doi.org/10.1039/B200372D>
- 410 4. Kerstel ERTh, Meijer HAJ. Optical isotope ratio measurements in hydrology (Chapter 9), in: Isotopes
411 in the water cycle: past, present and future of a developing science. pp. 109-124, P.K. Aggarwal, J. Gat,
412 and K. Froehlich (Eds.), IAEA Hydrology Section, Kluwer, 2005
- 413 5. Shine KP, Ptashnik IV, Raedel G. The water vapour continuum: brief history and recent developments.
414 Surv Geophys 2012;33:535-55. <https://doi.org/10.1007/s10712-011-9170-y>
- 415 6. Tretyakov MYu, Koshelev MA, Serov EA, Parshin VV, Odintsova TA, Bubnov GM. Water dimer and
416 the atmospheric continuum. Physics – Uspekhi, 2014;57:1083-98.
- 417 7. Serov EA, Odintsova TA, Tretyakov MYu, Semenov VE. On the origin of the water vapor continuum
418 absorption within rotational and fundamental vibrational bands. J Quant Spectrosc Radiat Transf
419 2017;193:1-12.
- 420 8. Partridge H, Schwenke DW. The determination of an accurate isotope dependent potential energy
421 surface for water from extensive *ab initio* calculations and experimental data. J Chem Phys
422 1997;106:4618-39.
- 423 9. Schwenke DW, Partridge H. Convergence testing of the analytic representation of an *ab initio* dipole
424 moment function for water: Improved fitting yields improved intensities. J Chem Phys 2000;113:6592-
425 7.
- 426 10. Polyansky OL, Zobov NF, Mizus II, Lodi L, Yurchenko SN, Tennyson J, et al. Global spectroscopy of
427 the water monomer. Phil Trans R Soc Lond A 2012;370:2728-48.
- 428 11. Polyansky OL, Kyuberis AA, Zobov NF, Tennyson J, Yurchenko SN, Lodi L. ExoMol molecular line
429 lists XXX: a complete high-accuracy line list for water. Mon Not R Astron Soc 2018;480:2597-608.
- 430 12. Gordon IE, Rothman LS, Hill C, Kochanov RV, Tan Y, Bernath PF, et al. The HITRAN2016 molecular
431 spectroscopic database. J Quant Spectrosc Radiat Transf 2017;203:3-69.
- 432 13. Jacquinet-Husson N, Armante R, Crépeau N, Chédin A, Scott NA, Boutammine C, et al. The 2015
433 edition of the GEISA spectroscopic database. J Mol Spectrosc 2016;327:31-72.
- 434 14. Kauppinen J, Karkkainen T, Kyro E. High-resolution spectrum of water vapor between 30 and 720 cm^{-1} .
435 J Mol Spectrosc 1978;71:15-45.
- 436 15. Partridge RH. Far-infrared absorption spectra of H_2^{16}O , H_2^{17}O , and H_2^{18}O . J Mol Spectrosc
437 1981;87:429-37.
- 438 16. Kauppinen J, Jolma K, Hornaman VM. New wave-number calibration tables for H_2O , CO_2 , and OCS
439 lines between 500 and 900 cm^{-1} . Appl Opt 1982;21:3332-6.
- 440 17. Johns JWC. High-resolution far infrared (20-350 cm^{-1}) spectra of several species of H_2O . J Opt Soc
441 Am B 1985;2:1340-54.
- 442 18. Matsushima F, Odashima H, Iwasaki T, Tsunekawa S, Takagi K. Frequency measurement of pure
443 rotational transition of H_2O from 0.5 to 5 THz. J Mol Structure 1995;352:371-8.
- 444 19. Paso R, Horneman VM. High-resolution rotational absorption spectra of H_2^{16}O , HD^{16}O , and D_2^{16}O
445 between 110 and 500 cm^{-1} . J Opt Soc Am B 1995;12:1813-37.
- 446 20. De Natale P, Lorini L, Inguscio M, Nolt IG, Park JH, Di Lonardo G, et al. Accurate frequency
447 measurements for H_2O and $^{16}\text{O}_3$ in the 119- cm^{-1} OH atmospheric window. Appl Opt 1997;36:8526-32.
- 448 21. Toth RA. Water vapor measurements between 590 and 2582 cm^{-1} : line positions and strengths. J Mol
449 Spectrosc 1998;190:379-96.
- 450 22. Chen P, Pearson JC, Pickett HM, Matsuura S, Blake GA. Submillimeter-wave measurements and
451 analysis of the ground and $\nu_2=1$ states of water. Astrophys J Suppl Series 2000;128:371-85.

- 452 23. Horneman VM, Anttila R, Alanko S, Pietila J. Transferring calibration from CO_2 laser lines to far
453 infrared water lines with the aid of the ν_2 band of OCS and the ν_2 , $\nu_1-\nu_2$, and $\nu_1+\nu_2$ bands of $^{13}\text{CS}_2$:
454 Molecular constants of $^{13}\text{CS}_2$. *J Mol Spectrosc* 2005;234:238-54.
- 455 24. Matsushima F, Tomatsu N, Nagai T, Moriwaki Y, Takagi K. Frequency measurement of pure rotational
456 transitions in the $\nu_2=1$ state of H_2O . *J Mol Spectrosc* 2006;235:190-5.
- 457 25. Cazzolli G, Puzzarini C, Buffa G, Tarrini O. Pressure-broadening of water lines in the THz frequency
458 region: Improvements and confirmations for spectroscopic databases. Part II. *J Quant Spectrosc Radiat*
459 *Transf* 2009;110:609-18.
- 460 26. Drouin BJ, Yu SS, Pearson JC, Gupta H. Terahertz spectroscopy for space applications: 2.5 – 2.7 THz
461 spectra of HD, H_2O and NH_3 . *J Mol Structure* 2011;1006:2-12.
- 462 27. Polyansky OL, Busler JR, Guo B, Zhang K, Bernath PF. The emission spectrum of hot water in the
463 region between 370 and 930 cm^{-1} . *J Mol Spectrosc* 1996;176:305-15.
- 464 28. Polyansky OL, Tennyson J, Bernath PF. The spectrum of hot water: rotational transitions and difference
465 bands in the (020), (100), and (001) vibrational states. *J Mol Spectrosc* 1997;186:213-21.
- 466 29. Polyansky OL, Zobov NF, Viti S, Tennyson J, Bernath PF, Wallace L. High-temperature rotational
467 transitions of water in sunspot and laboratory spectra. *J Mol Spectrosc* 1997;186:422-47.
- 468 30. Coudert LH, Pirali O, Vervloet M, Lanquetin R, Camy-Peyret C. The eight first vibrational states of
469 the water molecule: Measurements and analysis. *J Mol Spectrosc* 2004;228:471-98.
- 470 31. Coheur P-F, Bernath PF, Carleer M, Colin R, Polyansky OL, Zobov NF, et al. A 3000 K laboratory
471 emission spectrum of water. *J Chem Phys* 2005;122:074307.
- 472 32. Yu SS, Pearson JC, Drouin BJ, Martin-Drumel M-A, Pirali O, Vervloet M, et al. Measurement and
473 analysis of new terahertz and far-infrared spectra of high temperature water. *J Mol Spectrosc*
474 2012;279:16-25.
- 475 33. Winther F. The rotational spectrum of water between 650 and 50 cm^{-1} H_2^{18}O and H_2^{17}O in natural
476 abundance. *J Mol Spectrosc* 1977;65:405-19.
- 477 34. Kauppinen J, Kyro E. High resolution pure rotational spectrum of water vapor enriched by H_2^{17}O and
478 H_2^{18}O . *J Mol Spectrosc* 1980;84:405-23.
- 479 35. Guelachvili G, Rao KN. Handbook of infrared standards. Orlando FL: Academic Press; 1986.
- 480 36. Matsushima F, Nagase H, Nakauchi T, Odashima H, Takagi K. Frequency measurement of pure
481 rotational transitions of H_2^{17}O and H_2^{18}O from 0.5 to 5 THz. *J Mol Spectrosc* 1999;193:217-23.
- 482 37. Mikhailenko SN, Tyuterev VIG, Mellau G. (000) and (010) states of H_2^{18}O : analysis of rotational
483 transitions in hot emission spectrum in the 400 – 850 cm^{-1} region. *J Mol Spectrosc* 2003;217:195-211.
- 484 38. Toth RA. HDO and D_2O low pressure, long path spectra in the 600 – 3100 cm^{-1} region. I. HDO line
485 positions and strengths. *J Mol Spectrosc* 1999;195:73-97.
- 486 39. Janca A, Tereszchuk K, Bernath PF, Zobov NF, Shirin SV, Polyansky OL, Tennyson J. Emission
487 spectrum of hot HDO below 4000 cm^{-1} . *J Mol Spectrosc* 2003;219:132-5.
- 488 40. Mellau GCh, Mikhailenko SN, Tyuterev VIG. Hot water emission spectra: Rotational energy levels of
489 the (000) and (010) states of HD^{17}O . *J Mol Spectrosc* 2015;308-309:6-19.
- 490 41. Evenson KM, Jennings DA, Petersen FR. Tunable far-infrared spectroscopy. *Appl Phys Lett*
491 1984;44:576-8.
- 492 42. McKellar ARW. High resolution infrared spectroscopy with synchrotron sources. *J Mol Spectrosc*
493 2010;262:1-10.
- 494 43. Odintsova TA, Tretyakov Myu, Zibarova AO, Pirali O, Roy P, Campargue A. Far-infrared self-
495 continuum absorption of H_2^{16}O and H_2^{18}O (15-500 cm^{-1}). *J Quant Spectrosc Radiat Transf*
496 2019;227:190-200. <https://doi.org/10.1016/j.jqsrt.2019.02.012>
- 497 44. Odintsova TA, Tretyakov MYu, Simonova A, Ptashnik I, Pirali O, Campargue A. Measurement and
498 temperature dependence of the water vapor self-continuum in the 70–700 cm^{-1} range. *J Mol Structure*
499 2020;1210:128046. doi.org/10.1016/j.molstruc.2020.128046
- 500 45. Toureille M, Béguier S, Odintsova TA, Tretyakov MYu, Pirali O, Campargue A. The O_2 far-infrared
501 absorption spectrum between 50 and 170 cm^{-1} . *J Quant Spectrosc Radiat Transf* 2020;242:106709.
502 doi.org/10.1016/j.jqsrt.2019.106709

- 503 46. Coudert LH. Université Paris-Sud, private communication (2004).
 504 47. Barber RJ, Tennyson J, Harris GJ, Tolchenov RN. A high-accuracy computed water line list. *Mon Not*
 505 *R Astron Soc* 2006;368:1087-94.
 506 48. Lodi L, Tennyson J, Polyansky OL. A global, high accuracy *ab initio* dipole moment surface for the
 507 electronic ground state of the water molecule. *J Chem Phys* 2011;135:034113.
 508 49. Coudert L, Martin-Drumel M-A, Pirali O. Analysis of the high-resolution water spectrum up to the
 509 second triad and $J=30$. *J Mol Spectrosc* 2014;303:36-41.
 510 50. Lodi L, Tennyson J. Line lists for H_2^{18}O and H_2^{17}O based on empirical line positions and *ab initio*
 511 intensities. *J Quant Spectrosc Radiat Transf* 2012;113:850-8.
 512 51. Kyuberis AA, Zobov NF, Naumenko OV, Voronin BA, Polyansky OL, Lodi L, et al. Room temperature
 513 line lists for deuterated water. *J Quant Spectrosc Radiat Transf* 2017;203:175-85.
 514 52. Tennyson J, Bernath PF, Brown LR, Campargue A, Carleer MR, Császár AG, et al. IUPAC critical
 515 evaluation of the rotational-vibrational spectra of water vapor. Part I. Energy levels and transition
 516 wavenumbers for H_2^{17}O and H_2^{18}O . *J Quant Spectrosc Radiat Transf* 2009;110:573-96.
 517 53. Tennyson J, Bernath PF, Brown LR, Campargue A, Császár AG, Daumont L, et al. IUPAC critical
 518 evaluation of the rotational-vibrational spectra of water vapor. Part II. Energy levels and transition
 519 wavenumbers for HD^{16}O , HD^{17}O , and HD^{18}O . *J Quant Spectrosc Radiat Transf* 2010;111:2160-84.
 520 54. Tennyson J, Bernath PF, Brown LR, Campargue A, Császár AG, Daumont L, et al. IUPAC critical
 521 evaluation of the rotational-vibrational spectra of water vapor. Part III: Energy levels and transition
 522 wavenumbers for H_2^{16}O . *J Quant Spectrosc Radiat Transf* 2013;117:29-58.
 523 55. Tennyson J, Bernath PF, Brown LR, Campargue A, Császár AG, Daumont L, et al. IUPAC critical
 524 evaluation of the rotational-vibrational spectra of water vapor. Part IV: Energy levels and transition
 525 wavenumbers for D_2^{16}O , D_2^{17}O , and D_2^{18}O . *J Quant Spectrosc Radiat Transf* 2014;142:93-108.
 526 56. Yu SS, Pearson JC, Drouin BJ, Miller CE, Kobayashi K, Matsushima F. Terahertz spectroscopy of
 527 ground state HD^{18}O . *J Mol Spectrosc* 2016;328:27-31.
 528 57. Puzzarini C, Cazzoli G, Gauss J. The rotational spectra of HD^{17}O and D_2^{17}O : Experiment and quantum-
 529 chemical calculations. *J Chem Phys* 2012;137:154311.
 530 58. Lanquetin R, Coudert LH, Camy-Peyret C. High-lying rotational levels of water: an analysis of the
 531 energy levels of the five first vibrational states. *J Mol Spectrosc* 2001;206:83-103.
 532 59. Flaud J-M, Piccolo C, Carli B, Perrin A, Coudert LH, Teffo J-L, Brown LR. Molecular line parameters
 533 for the MIPAS (Michelson Interferometer for Passive Atmospheric Sounding) experiment. *Atmos*
 534 *Ocean Opt* 2003;16:172-82.
 535 60. Bubukina II, Zobov NF, Polyansky OL, Shirin SV, Yurchenko SN. Optimized semiempirical potential
 536 energy surface for H_2^{16}O up to 26000 cm^{-1} . *Opt Spectrosc* 2011;110:160-6.
 537 61. Kyuberis AA. Institute of Applied Physics RAS. Private communication (2016). Based on the updated
 538 database of energy levels from Ref. [52].
 539 62. *Ab initio* values from Ref. [50]
 540 63. Liu A-W, Du J-H, Song K-F, Wang L, Wan L, Hu S-M. High-resolution Fourier-transform
 541 spectroscopy of ^{18}O enriched water molecule in the $1080 - 7800\text{ cm}^{-1}$ region. *J Mol Spectrosc*
 542 2006;237:149-62.
 543